Core-Level Photoemission and LEED Studies of Adsorption at Fe Surfaces: Comparison Between CO and O₂

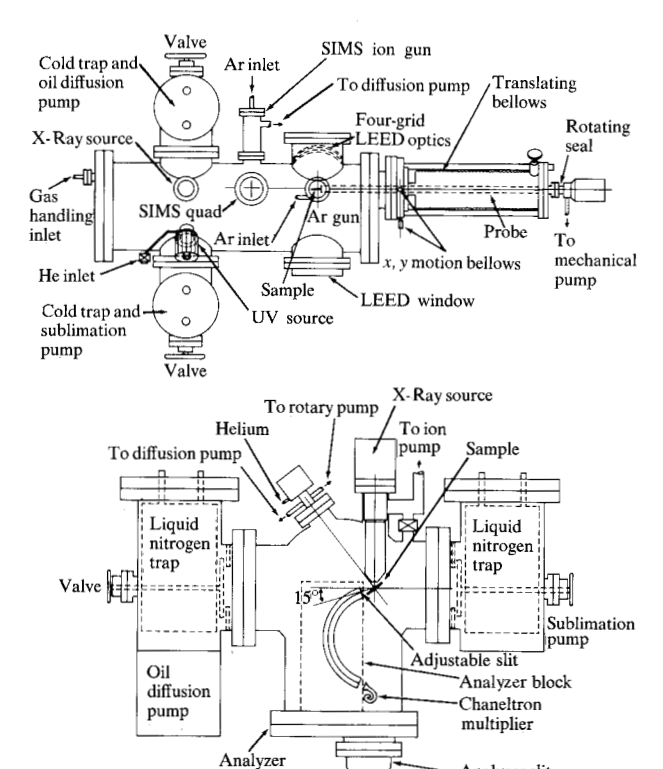
Abstract: Carbon monoxide and oxygen interactions with α Fe(100) and polycrystalline surfaces have been studied by x-ray photoemission (XPS or ESCA) and low energy electron diffraction (LEED) at temperatures between 123 K and 473 K. For CO, the XPS results demonstrate the existence of four electronically distinct CO adsorption states; one is dissociative and three are molecular. The binding energy analyses are consistent with one of the latter molecular adsorption states, formed on the polycrystalline surface, having a stretched CO bond compared with the equivalent state on the Fe(100) surface. For oxygen, only dissociative chemisorption is observed, even at 123 K. Assuming monolayer coverage at saturation allows calibration of the coverage for all other situations of CO and O_2 adsorption. It is demonstrated that at coverages of just greater than a monolayer (293 K adsorption), Fe oxide species are already present and that Fe^{III} dominates. Studies at grazing angles, designed to enhance the surface sensitivity of the core-level measurements, fail to reveal recognizable Fe^{II} or Fe^{III} species much below monolayer coverage even though LEED studies indicate that an FeO-like geometric structure has developed at coverages much lower than this.

Introduction

Chemisorption and initial oxidation studies of transition metal and alloy surfaces may be important to the basic understanding of three phenomena: corrosion, catalysis, and thin film magnetism. A large gap exists between the "corrosion scientist" for whom air-exposed metal surfaces covered with a variety of reaction products to depths of one to ten nm are the starting point of studies that consume additional microns of material [1], and the "surface physicist" who starts with clean single-crystal surfaces and stops his chemisorption studies at the monolayer coverage point [2(a)]. It is entirely unclear, because of a lack of attempts to link the two fields, whether the chemisorption and initial oxidation processes have any influence on subsequent heavy corrosion. It is also not clear whether an understanding of the one area will assist in developing an understanding of the other. Practical heterogeneous catalysts are usually transition metals and alloys dispersed as small particles on a support material (e.g., Al₂O₃) [2(b)]. They may be treated to some mysterious "activation" processes before use. The object of the catalyst is to increase the reaction rate, or, more importantly, the selectivity of a reaction toward a desired product [2(b)]. Reactions are usually performed with the reactants at high pressure. The relevance of chemisorption studies performed on clean surfaces under ultra high vacuum (UHV) conditions to catalysis then rests on the assumption that an understanding of reaction mechanisms on such surfaces can be correlated with those on practical catalyst surfaces. In specific cases, if not in general, this is probably true. Note, for example, the deactivation of surfaces toward specific reactions through contamination by sulfur, carbon, etc. [3, 4]; or the phenomenon of "surface reorientation" [5], where it has been claimed that the different geometries of a single-crystal surface and the equivalent catalytic particle surface are both reoriented by adsorption to a common structure. In thin film technology two aspects must be considered. First, even very mild corrosion consumes a significant fraction of the material if the films are very thin; and second, for some thin film alloys it is conceivable that a highly reactive component may exist in an oxidized form throughout the film, causing unexpected effects on the magnetic properties [6].

The increase in experimental activity in the area of chemisorption bonding over the last decade has been accompanied by a similar increase in theoretical activity [2(c)]. Models for the interaction of the CO molecule and the oxygen atom with metal surfaces have been considered [7-11], the usual links to experiment being made through ultraviolet (UV) photoemission and LEED re-

Copyright 1978 by International Business Machines Corporation. Copying is permitted without payment of royalty provided that (1) each reproduction is done without alteration and (2) the *Journal* reference and IBM copyright notice are included on the first page. The title and abstract may be used without further permission in computer-based and other information-service systems. Permission to *republish* other excerpts should be obtained from the Editor.



Analyzer slit

manipulator

Figure 1 Electron spectrometer block diagram.

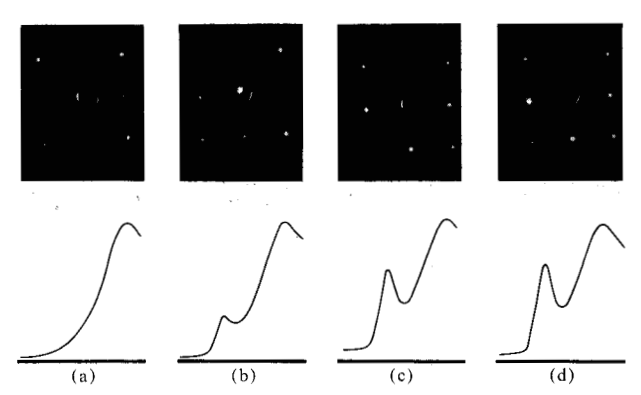


Figure 2 Low energy electron diffraction (LEED) (92 eV) for CO adsorption on Fe(100): (a) clean surface, (b)-(d) at CO exposures corresponding to the O(1s) XPS intensities indicated schematically. The maximum exposure required to saturation (d) was approximately 4×10^{-4} Pa-s (3 langmuirs).

sults. The CO/Ni system is perhaps the best example of the former experiments. Here the original experimental assignment of the CO "orbital resonances" observed in the photoemission spectrum changed [12, 13] as a result of comparison with theoretical electronic structure calculations on Ni/CO cluster models and with both theoretical calculations [7, 11] and photoemission measurements on transition metal carbonyl compounds (see comments of D. R. Lloyd in [12]). Along with the reassignment came an appreciation of the significant reduction in observed orbital energies caused by electron reorganization (relaxation) under the influence of the positive hole of the photoionization final state. Ultraviolet photoemission work on hydrocarbon adsorption had also demonstrated this effect [14]. Subsequently, more sophisticated photoemission measurements involving variation of the photon energy (synchrotron radiation) confirmed the necessity for a reassignment [15]. Since that time both angle-resolved, polarization-dependent and variable $h\nu$ data have been used to establish the orientation of the CO molecule with respect to metal surfaces [16–18].

For LEED there is now a substantial body of data providing determination of the geometry of *ordered* O, S, and N atoms on single-crystal surfaces that can be compared with the predictions of theory [19].

Though UV photoemission studies combined with LEED have assisted greatly in elucidating the electronic and geometric nature of chemisorption bonding, they do have some serious deficiencies that one can attempt to overcome by using other surface techniques. Low energy electron diffraction provides no information about disordered species, and it can be very difficult to even establish whether a major, or only a minor, portion of the adsorbate is in the ordered structure giving rise to a LEED pattern. Ultraviolet photoemission does not provide a good quantitative elemental analysis of the surface. In addition, detection and interpretation of multiple adsorption states, either of the same molecule or of a combination of molecules, are difficult because of the possibility of strongly overlapped features and the often unpredictable changes in valence energy levels with change in adsorption bonding characteristics [2(d)].

Studying the core levels by x-ray photoemission (XPS) provides one means of helping overcome the deficiencies mentioned previously. Since the core levels are essentially atomic in nature, relative intensity measurements can provide a more quantitative analysis than UV photoemission. Core-level chemical shifts, while not giving the direct bonding information of the valence levels, provide a surer means of distinguishing among different adsorption states. In addition, since the shifts for each type of atom in an adsorbed molecule can be monitored, interpretation in terms of bonding characteristics can sometimes be simpler than for UV photoemission [2(d)]. It is, of course, true that a combined electron emission study encompassing valence levels, core levels, and Auger electrons (which may provide further information from their chemical shifts) is ideal for electron spectroscopy.

The work described in this paper involves simultaneous XPS and LEED measurements of the adsorption of CO

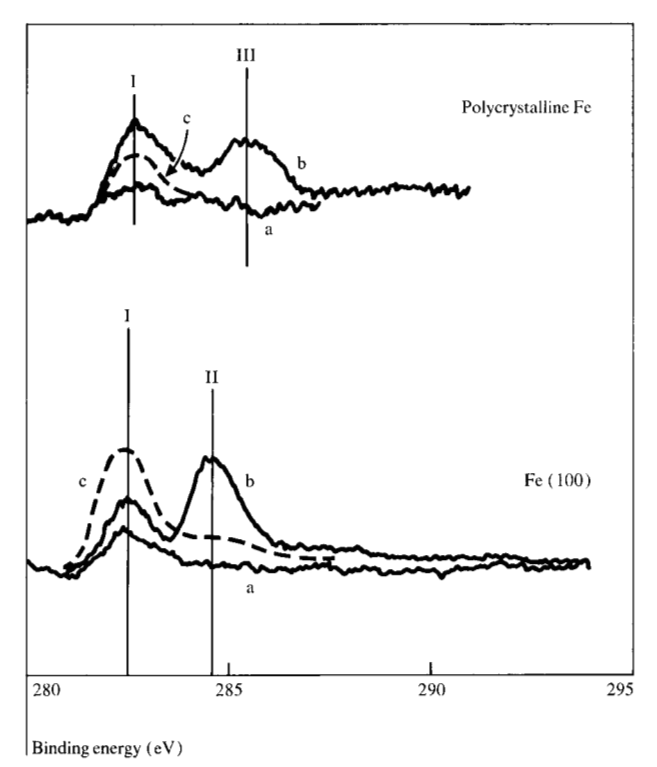
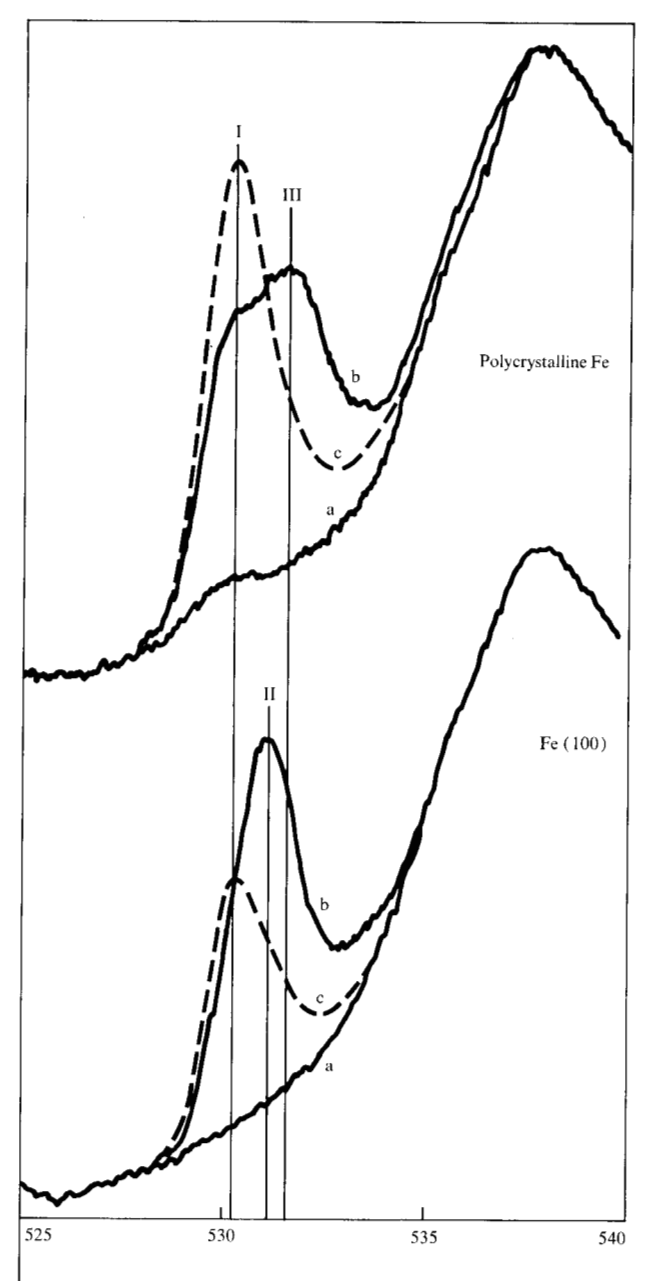


Figure 3 C(1s) XPS spectra (recorded at 20 eV analyzer bandpass energy, 300 s recording time, 1 s time constant) for the adsorption of CO on Fe at 293 K. Traces are for (a) clean Fe surface, (b) saturation CO coverage, and (c) surface warmed to 373 K.

and oxygen on an α Fe(100) surface. UV photoemission measurements were also carried out, but they will not be discussed here. X-Ray photoemission spectroscopy (XPS) measurements on a polycrystalline surface were also made. Studies of Fe surfaces have obvious implications for corrosion studies. Nickel-iron-based alloys are extensively used in thin-film and other magnetic devices and are also being investigated as potential catalyst materials. We are extending the present studies to single-crystal NiFe alloys. The choice of oxygen as an adsorbate is obvious in relation to oxidation and corrosion, and follows from earlier work by the present author and coworkers on Fe films [20, 21]. It was decided to study CO in detail because of the extensive photoemission and theoretical literature available for CO adsorption on other transition metal surfaces and because it has been reported that Fe occupies a borderline position with respect to those transition metals that cause CO dissociation and those that do not [17].

Experimental procedure

The spectrometer system used in these studies was specially constructed by V. G. Scientific, East Grinstead, U.K. A block diagram is given in Fig. 1. It is an UHV



Binding energy (eV)

Figure 4 O(1s) XPS spectra (20 eV, 300 s recording time, 1 s time constant) for the adsorption of CO on Fe at 293 K. Traces represent (a) the clean Fe surface, (b) the saturation CO coverage, and (c) the spectra after flash heating to 373 K for a few seconds.

diffusion- and sublimation-pumped system (base pressure $<9\times10^{-9}$ Pa) which has facilities for XPS (Al K α and Mg K α twin-anode 1486-eV and 1256-eV energy). He I and He II photoemission (21.2 eV and 40.8 eV), LEED, electron impact Auger, and secondary ion mass spectrometry (SIMS).

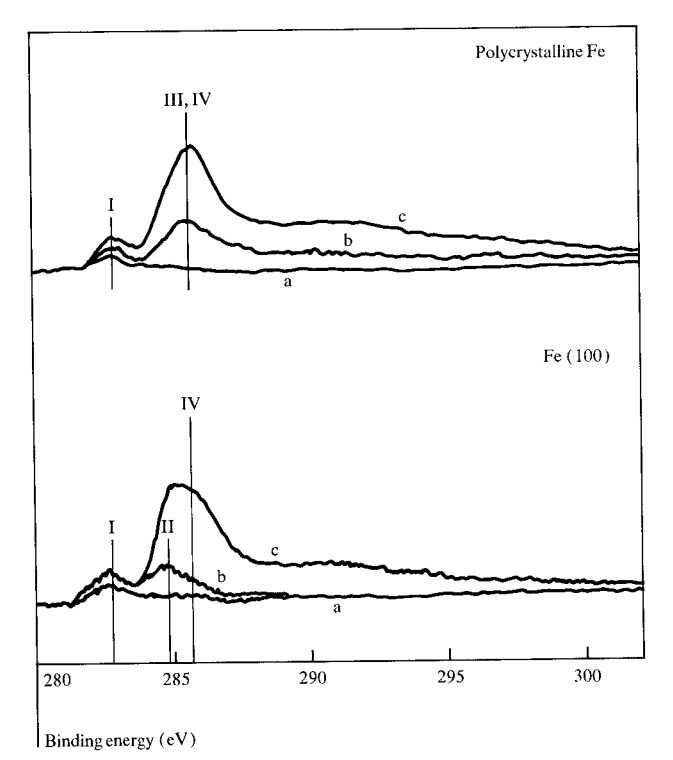


Figure 5 C(1s) XPS spectra for the adsorption of CO on Fe at 123 K (20 eV, 300 s recording time, 1 s time constant). Traces represent (a) clean surface, (b) initial adsorption, and (c) saturation coverage.

The high resolution analyzer used for the XPS/UPS analysis is of the hemispherical type [22]. The LEED optics are of standard four-grid design. The sample may be cooled by circulation of liquid nitrogen through the sample probe and heated by electron bombardment or direct current. The probe is fully rotatable so that polar angle variation is available for both UPS and XPS. A separate UHV gas handling system is connected to the spectrometer for the introduction of adsorbates.

The cut and polished α -Fe crystal measured 1 cm \times $1 \text{ cm} \times 0.1 \text{ cm}$ and was oriented to within one degree of (100). It was attached to the sample probe by spotwelding the edges to 0.5-mm tungsten rods. Temperatures of ~123 K could be obtained in the liquid nitrogen cooling mode. Cleaning the crystal proved extremely difficult, as has been found previously for Fe single-crystal surfaces [23, 24]. The main problems encountered were the restriction to temperatures below the phase transition (1185 K) and the rather large bulk carbon content of the single crystals. It has been found that repeated cycles of Ar ion bombardment at 1073 K followed by 673 K (12 hours each) plus a final flash anneal to ≈973 K is capable of producing a surface free from oxygen and nitrogen and largely free from carbon. To avoid excessive sputtering of the iron, bombardment by H⁺ ions may also be used in

the final cleaning cycles. The nitrogen apparently only segregates to the surface once the carbon content of the bulk (or subsurface) has been reduced enough that it does not segregate to the surface in large quantities. Thus nitrogen was not observed in the early stages of cleaning. No sulfur impurities were observed during this study. The whole cleaning treatment takes about one week and even then the residual carbon constitutes about 8% coverage if the carbon were all present right at the surface. Because it is more likely to be spread over several layers this figure represents a maximum contamination level. The Fe(2p):C(1s) relative intensities from which the contamination estimate was made (discussed later) are 1:0.003 at this point. The LEED spectrum of such a surface showed sharp (1×1) spots with no evidence of any overlayer $c(2\times 2)$ structure, at any voltage [Fig. 2(a)]. The LEED data on deliberately contaminated surfaces, or earlier in the cleaning cycle, show that C, N, or O all form $c(2\times2)$ patterns. The clean surface could be kept for about one hour at the best base pressure before faint $c(2\times2)$ spots began to appear. At higher base pressure, the "clean time" was shorter and we believe the $c(2\times2)$ pattern is caused by residual CO, which as we shall see later is initially adsorbed in a dissociated form. Though we have the small amount of residual carbon on the "clean" surface, the state of cleanness is considerably better than in the α Fe(100)/O₂, study of Dwyer and Simmons [23], where $c(2\times 2)$ spots are clearly evident on their "clean" surface, and it is comparable to that in the study of Brucker and Rhodin [24].

The Fe polycrystalline surfaces were prepared by Ar⁺ sputtering clean ordered surfaces until no diffraction pattern was observable. The subsurface does, of course, contain some occluded argon under these conditions.

Adsorption runs were carried out both dose-wise and continuously while XPS and LEED data were recorded. Pressure measurements were made by nude ion gauge. Adsorption runs were carried out with the gauge both on and off; no effects due to the ion gauge were observed. These measurements are uncorrected and so the quoted exposures are nominal. Mg $K\alpha$ radiation (1256 eV) was used mainly because higher fluxes were obtainable and because slightly shorter escape depths are involved than for Al $K\alpha$ (1486 eV). Unless otherwise stated, the electron ejection angle ϕ (Fig. 1) was set at 45° for all XPS spectra.

Results

Figures 3 and 4 show the C(1s) and O(1s) XPS regions for Fe(100) in the as-cleaned state, at saturation coverage of CO at 293 K and after flash heating to about 373 K for a few seconds. Flashing to 973 K reproduced the original clean state. The binding energy (BE) scale is calibrated against the Fe(2p_{3/2}) line of the clean iron at 707.0 eV,

which suffers no significant change during the adsorption other than a slight intensity decrease. The additional structure in the O(1s) spectra is due to an Fe Auger line. It can be eliminated by using Al $K\alpha$ radiation instead of Mg $K\alpha$, but in fact provides a useful internal intensity standard.

The LEED patterns (92 eV) observed at various stages up to saturation are shown in Figs. 2(b)–(d), together with a schematic of the equivalent XPS O(1s) spectra. The flash heating to 373 K of the saturated surface produced a slight increase in the intensity of the $c(2\times2)$ spots and an increase in the intensities of the four spots nearest the 0, 0 beam. However, even at this point, the $c(2\times2)$ spots are not very sharp or intense in contrast to the situation of a deliberately heavily contaminated surface (C, N, or O) that has been well annealed. In the latter situation all spots are sharp and of approximately equal intensity at 92 eV.

Figures 3 (upper) and 4 (upper) show the C(1s) and O(1s) spectra for adsorption on the Fe polycrystalline surface. Figures 5 and 6 show the C(1s) and O(1s) spectra obtained for adsorption at 123 K on the (100) and polycrystalline surfaces at an intermediate and saturation coverage stage. Low energy electron diffraction data were recorded in the low temperature study only at saturation coverage. At 92 eV no $c(2\times2)$ spots could be observed, just the original (1×1) pattern with rather a high background. Faint $c(2\times2)$ spots could be observed at higher voltages.

The relative intensities of the XPS C(1s), O(1s), and $Fe(2p_{3/2})$ lines, measured by area, for saturation coverages at 123 K and 293 K are given in Table 1, together with coverage estimates derived from these ratios (see discussion section).

Figure 7 shows the growth of the O(1s) peak, taken at an ejection angle of 45°, for the Fe(100) surface at 293 K exposed to oxygen. At an exposure of 28.3×10^{-4} Pa-s (21.3 langmuirs), the fast stage of the reaction is complete; a further 26.6×10^{-4} Pa-s (20-langmuir) exposure produced insignificant change in the spectrum. No significant shift or change in half-width was observed for the O(1s) peak as a function of exposure. Figures 8 and 9 show the changes occurring in the $Fe(2p_{3/2, 1/2})$ spectra at $\phi = 45^{\circ}$ and 20°, respectively, during the oxygen reaction. Several recent LEED studies of the adsorption of O₉ on Fe(100) have been reported [23-25]. The behavior we observe (Fig. 10) is consistent with these recent reports, rather than with earlier reports where the cleanness of the surface was in doubt. A $c(2\times2)$ pattern is observed immediately on adsorption, which reaches its maximum intensity (92 eV) at around 1.3×10^{-4} Pa-s (1-langmuir) exposure. The $c(2\times2)$ spots, which are never very strong, fade rapidly beyond this point, and by 8×10^{-4} Pa-s (6 langmuirs), the pattern returned to (1×1) , with the four

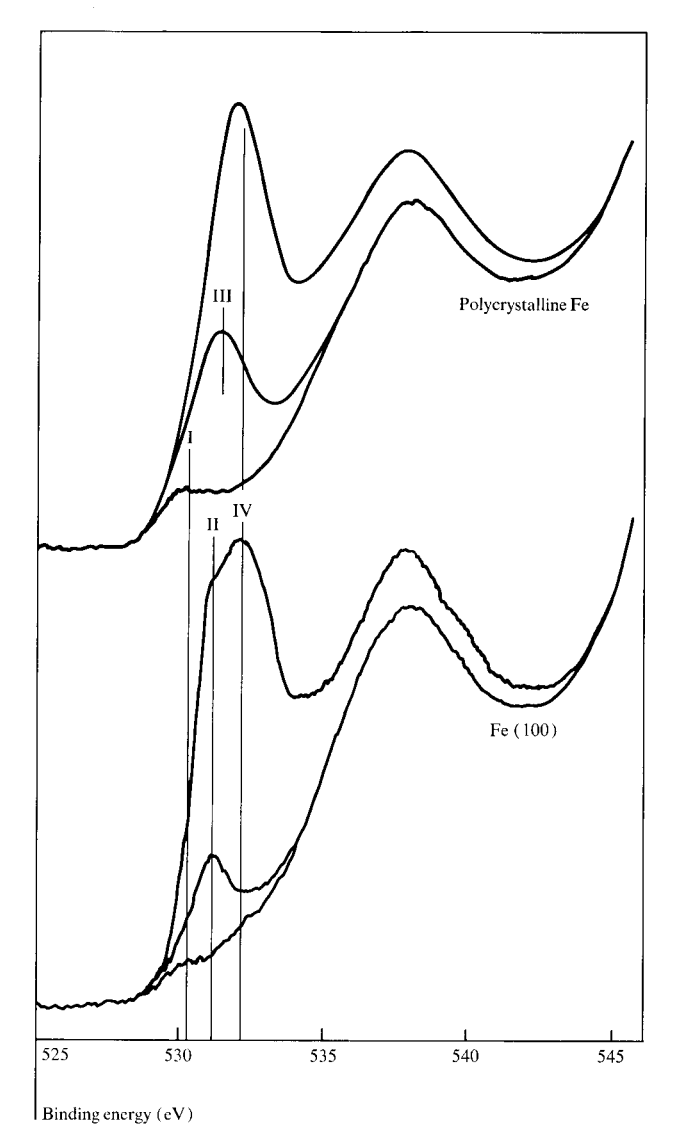


Figure 6 O(1s) XPS spectra for the adsorption of CO on Fe at 123 K (20 eV, 300 s recording time, 1 s time constant) for (a) clean surface, (b) initial adsorption, and (c) saturation coverage.

spots nearest the 0, 0 beam being very intense and fuzzy and the remaining spots being weak and sharp [Fig. 10(b)]. This pattern has previously been ascribed to a two-dimensional layer of FeO with epitaxial relationship to the substrate and a lattice parameter slightly smaller than that for bulk FeO, thus accounting for the coincidence between substrate and FeO overlayer lattice reflections [23]. Further exposure to oxygen gradually weakens all features until by 12.4×10^{-4} Pa-s (9.3-langmuir) exposure, for which the equivalent O(1s) spectrum is recorded in Fig. 7, only a very faint (1×1) is observable [Fig. 10(c)] and by 20×10^{-4} Pa-s (15 langmuirs) only a high background is observable [Fig. 10(d)].

Figure 11 shows the O(1s) spectra for saturation coverage for exposure at 123 K and the result of subsequent

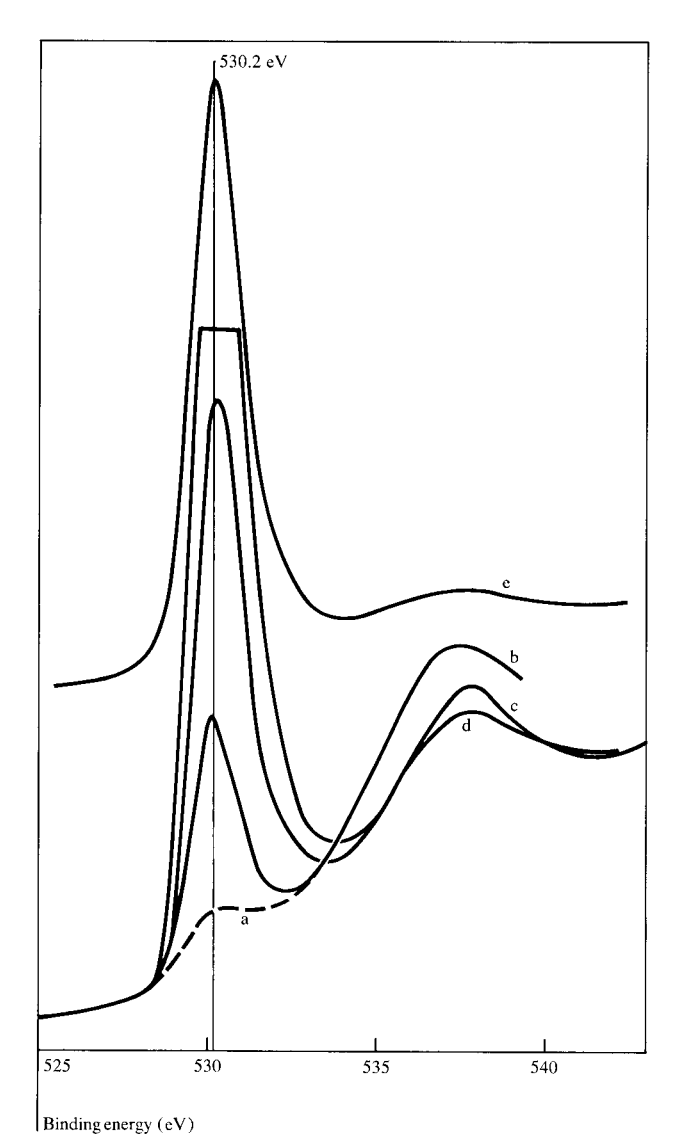
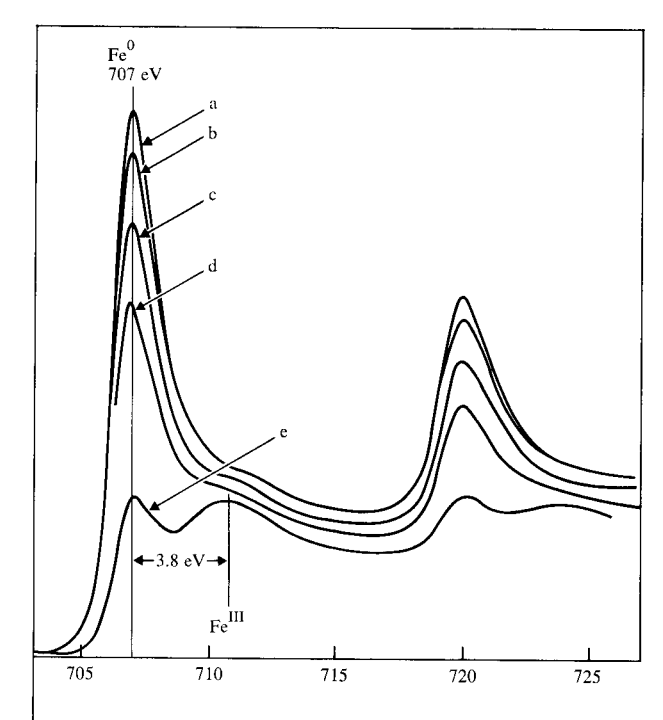


Figure 7 Growth of O(1s) peaks as a function of exposure to O_2 (in 10^{-4} Pa-s and parenthetically in langmuirs) for the Fe(100) surface at 293 K. Traces represent (a) clean surface, (b) 3 (2.3), (c) 12.4 (9.3), (d) 20 (15), and (e) 28.3 (21.3). Spectra were recorded at 20 eV analyzer bandpass energy in 300 s with a time constant of 1 s. Trace (e) has been scaled down by a factor of 3.3.

warming to 293 K. Both Mg K α - and Al K α -induced spectra are shown because of the complication of additional structure around 534 eV at 123 K.

Low energy electron diffraction shows no evidence for the formation of a $c(2\times2)$ pattern during adsorption of oxygen at 123 K. (In the present work, a *very* weak $c(2\times2)$ observable only at voltages higher than 92 eV was present *before* the addition of the first dose of oxygen. This we ascribe to the dissociation of residual CO during cooling from 973 K to 123 K.) At 92 eV all that was observed, in contrast to the 293-K case, was rapid increase and then



Binding energy (eV)

Figure 8 Fe($2p_{3/2,\ 1/2}$) spectra as a function of exposure to O_2 for the Fe(100) surface at 293 K in 10^{-4} Pa-s (langmuirs). Traces represent (a) clean surface, (b) 7 (5.3), (c) 12.4 (9.3), (d) 20.3 (15.3), and (e) 28.3 (21.3). (20 eV, 300 s recording time, 1 s time constant).

decrease in background intensity as a function of exposure to leave at saturation the $p(1\times1)$ pattern supposedly characteristic of an FeO layer.

The O(1s) and Fe($2p_{3/2}$) relative intensities at various points during the adsorption at 293 K and 123 K are given in Table 1, together with coverage estimates.

Discussion

• Analytical aspects

The coverage estimates in Table 1 were obtained from the relative $Fe(2p_{3/2})$ and O(1s) or C(1s) intensities by the following procedure.

The fraction I_d of the total clean surface $Fe(2p_{3/2})$ intensity I_0 , originating from the top layer of atoms, was obtained from the relationship

$$I_d = I_0(1 - \exp^{-d}/L_e \sin \phi),$$
 (1)

where d is the α Fe interlayer spacing normal to the (100) surface (0.143 nm), $L_{\rm e}$ is the escape depth for 550-eV electrons through iron, and ϕ is the angle of ejection of the detected electrons. A value of $L_{\rm e}=0.7$ nm was used [26], yielding an I_d value of 25 percent. Thus, the measured ratio O(1s):Fe(2p_{3/2})_{clean} when multiplied by 4σ

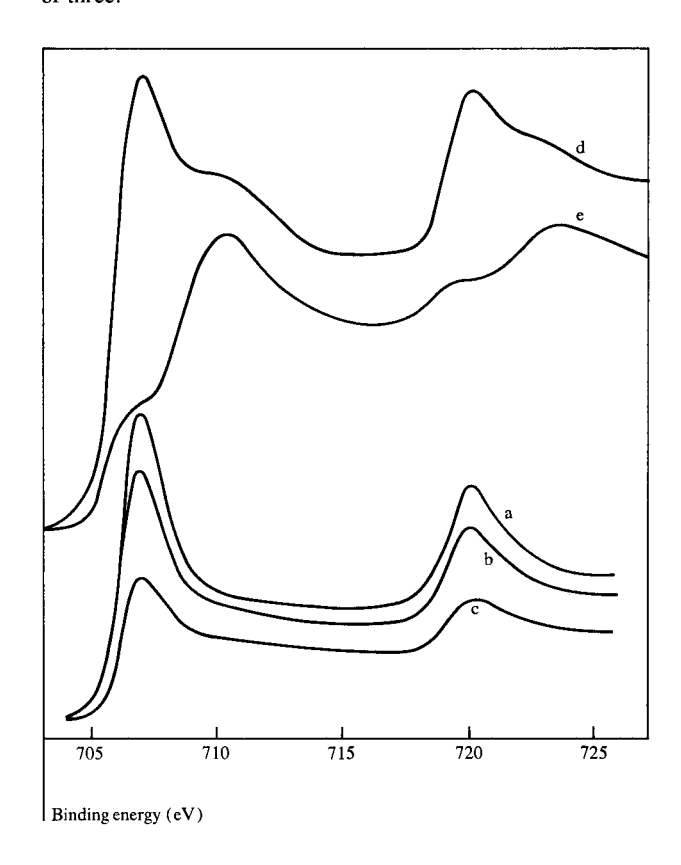
Table 1 Relative XPS intensities^a of C(1s) and O(1s) lines and derived surface coverage.

Surface and adsor- bant conditions	Temperature (K)	Peak intensity		Coverage θ , estimated from ^b		Relative ^c θ value
		O(1s)	C(1s)	O(1s)	C(1s)	
Fe(100), CO, saturated	293	0.025	0.010	0.38	0.43	0.20
Fe(100), CO, saturated	123	0.077	0.029	1.13	1.20	0.61
Polycrystalline Fe, CO, saturated	293	0.029	0.009	0.44	0.39	0.23
Polycrystalline Fe, CO, saturated	123	0.083	0.031	1.26	1.33	0.68
$Fe(100), O_2, 2.3 L^d$	293	0.028	_	0.41	_	0.22
Fe(100), O ₂ , 15 L	293	0.115		1.67		0.90
Fe(100), O ₂ , saturated	293	0.211	_	3.12	_	1.68
Fe(100), O ₂ , saturated	123	0.125		1.85	_	1.00

[&]quot;Intensities measured by area for saturation coverages at 123 K and 293 K; intensities given relative to the Fe(2p32) line for the clean iron surface.

 $Fe(2p_{3/2})/\sigma O(1s)$, where σ is the photoionization cross section for $h\nu = 1256 \text{ eV}$, represents the coverage in terms of oxygen atom monolayers (defined as one adsorbed atom per surface Fe atom). A similar calculation can be performed by using the C(1s) intensities and σ C(1s) [27] to yield carbon atom monolayers. These are the values shown in Table 1, columns 5 and 6, the values for σ being taken from atomic cross-section tables of Scofield [27]. The absolute coverages calculated in this manner are unlikely to be reliable to better than 50 percent because of several uncertainties in the parameters used. The electron escape depth $L_{\rm e}$ is not known with confidence, despite recent work in this area [28-30]. The relative atomic cross sections of Scofield [27] are expected to be accurate to within 10 percent. There are two experimental complications. The first is the actual measurement of the relative areas of the photoemission peaks. It is well recognized [2(d)] that it is difficult to partition intensity between signal and scattered electron background, especially when there might be genuine multiplet or shake-up structure following a photoelectron peak which should be included as part of the peak intensity. Secondly, a correction of the measured intensities should be made to allow for the transmission function of the spectrometer, which varies with kinetic energy (KE). It is these factors which probably cause the coverage estimate using the C(1s) intensities to differ slightly from those using the O(1s) intensities in the CO adsorption cases rather than any departure from a 1:1 relative intensity of carbon to oxygen atoms. The relative coverages for all adsorption situations of Table 1 should be much more accurate, since

Figure 9 Fe($2p_{3/2, 1/2}$) spectra at an electron ejection angle ϕ of 20° as a function of exposure to O_2 for the Fe(100) surface at 293 K. Traces are for (a) clean surface, and exposures (in 10^{-4} Pa-s and parenthetically in langmuirs) of (b) 7 (5.3), (c) 12.4 (9.3), (d) 20.3 (15.3), and (e) 28.3 (21.3). (20 eV, 300 s recording time, 1 s time constant). Traces (d) and (e) have been scaled up by a factor of three.



bCoverages estimated from an L_e value of 0.7 nm, and σ values taken from Scofield [27]

eValues given relative to the θ for Fe(100) for O₂ saturation at 123 K.

dA langmuir (L) is a measure of exposure representing 1.33 × 10⁻⁴ Pa-s, e.g., an exposure of 1.33 × 10⁻⁴ Pa (10⁻⁶ torr) for 1 second, 1.33 × 10⁻⁵ Pa for 10 seconds, etc.

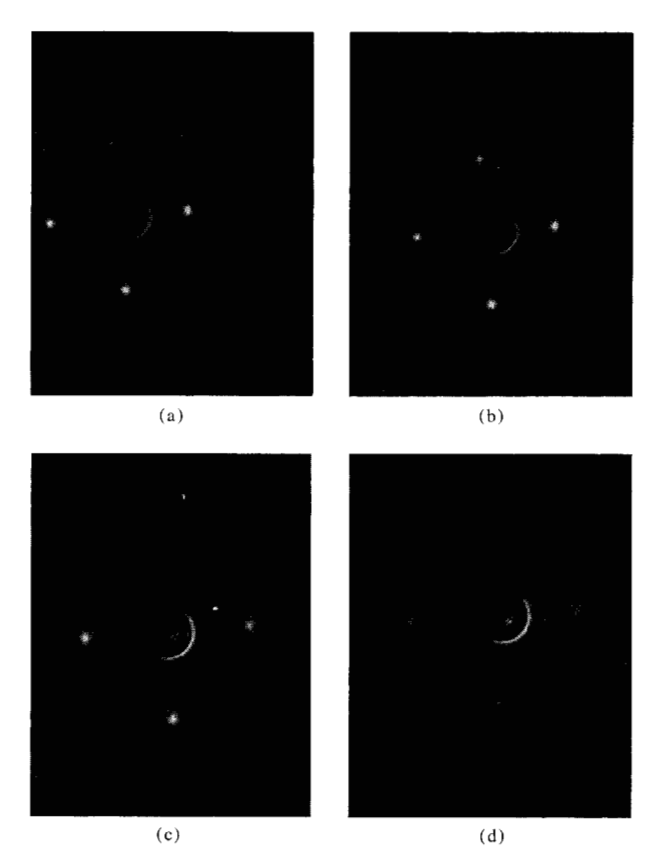


Figure 10 Low energy electron diffraction patterns (92 eV) for O_2 adsorption on Fe(100) at various exposures, given in 10^{-4} Pa-s and parenthetically in langmuirs. (a) 3 (2.3), (b) 7 (5.3), (c) 12.4 (9.3), and (d) 20 (15).

these are not affected by transmission function or by inaccuracies in $L_{\rm e}$ and σ . The last column of Table 1 is, therefore, a normalization of the intensities to unity for saturation O_2 adsorption on Fe(100) at 123 K. The choice of unity is arbitrary but reasonable, since there is evidence that for O_2 adsorption on Fe films at 77 K saturation coverage is one monolayer [31]. A calibration by flash desorption would be useful for CO adsorption. For O_2 adsorption oxygen dissolves into the bulk on heating. The estimates are likely to be more accurate than any based on "full" development of a LEED pattern, which are notoriously unreliable since they assume that only perfect ordering exists and that there is a one-to-one relationship between LEED spot intensity and coverage.

The values of the derived coverages in Table 1 are discussed later with respect to the observed LEED changes and the information provided by the binding energy analysis.

• Oxygen adsorption: BE and LEED analyses

We have previously reported XPS and UPS data concerning the adsorption of oxygen on Fe films [20], and on the XPS spectra of well characterized bulk Fe oxides [21]. The object of the latter, aside from intrinsic interest in the electronic structure of the oxides, was to use the characteristic spectra to "fingerprint" the results of the Fe/O, interactions and so determine, if possible, which Fe oxide species are formed during early oxidation. We were able to establish from the oxide studies that Fe³⁺ species are distinguishable from Fe2+, both in the 2p core level and the valence band, but octahedral coordination is not easily distinguishable from tetrahedral coordination. The Fe(2p_{3/2}) spectra of Fe metal FeO, Fe₂O₃, and Fe₃O₄ are shown in Fig. 12. We were then able to identify Fe³⁺ as the dominant species formed at high coverage θ (>1.5) on oxidation of polycrystalline iron, but could not rule out the possibility of Fe2+ being present as a minor constituent (Fe₃O₄ or Fe₂O₃ could therefore be the product). A typical oxidized film Fe(2p_{3/9}) spectrum is also shown in Fig. 12. We were also able to show that the valence band spectra, by XPS or UPS, were characteristic of Fe³⁺ as the major species. This is in disagreement with an earlier interpretation of very similar UPS data [24] where an assignment to FeO was made. At lower oxygen coverages a clear chemically shifted Fe(2p_{3/9}) peak was not observed, making identification of the species formed impossible. The reason for the lack of a shifted peak could be either that no species resembling Fe²⁺ or Fe³⁺ is formed, or that the escape depth is too great to allow resolution of a small chemically shifted component from the unshifted substrate peak.

In the present work we have repeated the adsorption measurements on the Fe(100) surface, the Fe(2p_{3/9}) results at $\phi = 45^{\circ}$ being shown in Fig. 8. The major product at the saturation stage, as judged by the 3.8-eV shift observed between the oxidized overlayer and the substrate $Fe(2p_{3/2})$ signals [trace (e)], is clearly identified as Fe^{3+} . The lower exposure spectra show no clear evidence for a chemically shifted component. In Fig. 9 at $\phi = 20^{\circ}$, the effective escape depth is reduced [Eq. (1)]. There is, as expected, a large increase in the ratio of Fe oxide to Fe metal for trace (e), and, more importantly, it becomes clear that trace (d), the 20.3×10^{-4} Pa-s (15.3-langmuir) exposure case, exhibits clear evidence of Fe³⁺. From the last column of Table 1, the 20.3×10^{-4} Pa-s exposure case corresponds to $\theta = 0.9$ and at $\phi = 20^{\circ}$, ≈ 45 percent of the Fe signal should originate from the outermost layer [Eq. (1)]. A rough deconvolution of trace (d), Fig. 9, into Fe⁰ and Fe³⁺ (or Fe³⁺/Fe²⁺) components indicates that around 0.8 of this outer layer of Fe atoms has been converted to Fe^{3+} (+ Fe^{2+}); i.e., at $\theta = 0.9$ oxygen coverage, a genuine oxide layer exists. The 12.4×10^{-4} Pa-s (9.3langmuir) exposure corresponds to $\theta = 0.55$ and there-

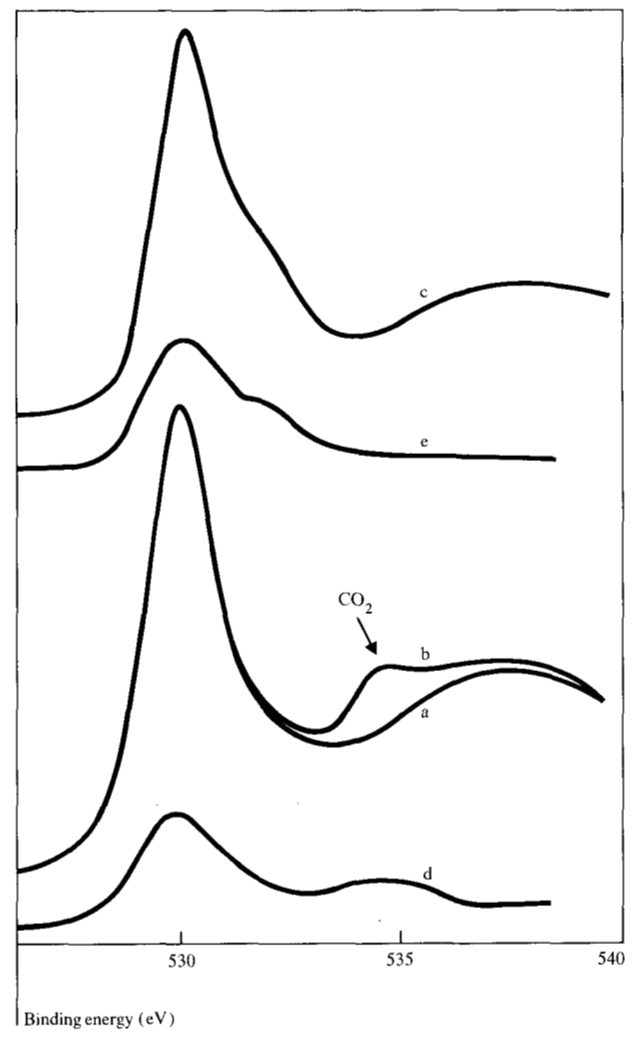


Figure 11 O(1s) spectra produced with Mg K α radiation for saturation adsorption of O₂ on Fe(100) at 123 K. (a) initial spectrum, (b) after 10 min in O₂ at an exposure of $\approx 40 \times 10^{-3}$ Pa-s (300 langmuirs), and (c) after warming to 293 K. Traces (d) and (e) are similar to (b) and (c), except that they were produced with Al K α radiation.

fore, at $\phi=20^\circ$, some 25 percent of the Fe signal should be chemically shifted if the bonding characteristics are the same as for the $\theta=0.9$ case. We would expect to see evidence for this in Fig. 9, trace (c), which is not the case. The conclusion is that whereas at around monolayer coverage an oxide layer is present with Fe³⁺ dominant, at half-monolayer coverage the oxygen atoms do not significantly perturb the electronic structure of the surface Fe atoms. An explanation of this phenomenon would be that nucleation of three-dimensional oxide islands (of sufficiently large macroscopic size for the Fe atoms to be electronically equivalent to the Fe³⁺ core of a bulk oxide) becomes significant only above $\theta=0.5$. Chemisorbed oxygen

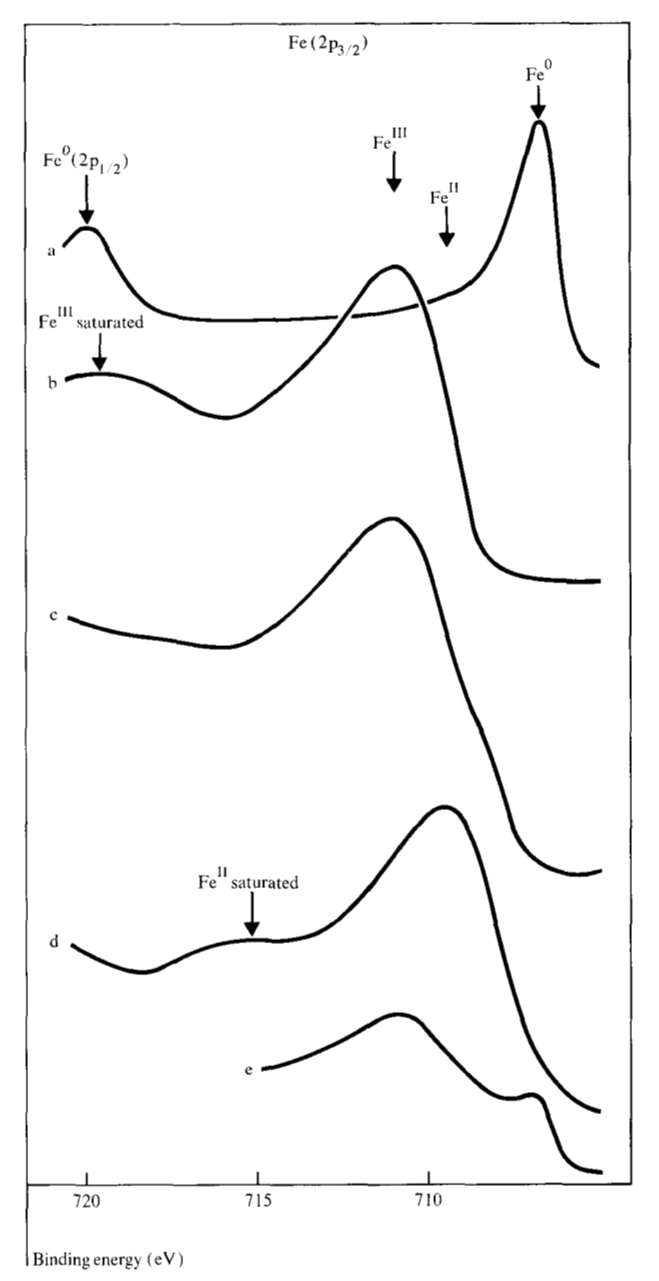


Figure 12 Fe $(2p_{3/2})$ XPS spectra for (a) an Fe foil, (b) Fe $_2O_3$, (c) Fe $_3O_4$, (d) FeO, and (e) an oxidized polycrystalline Fe foil. Spectra were recorded on a Hewlett-Packard 5950A, with monochromatized Al K α radiation [21].

gen not present in the island must not produce any significant alteration in the metallic electronic state of the neighboring Fe atoms. The O(1s) signal, with the binding energy (BE) of 530.2 eV, however, is characteristic of O^{2-} or something close to this *right from the start* of adsorption. An O(1s) BE of ≈ 530 eV is observed for FeO,

 Fe_2O_3 , Fe_3O_4 , and a number of other ionic metal oxides [2(d)]. There is no evidence for any significant concentrations of molecular oxygen (which would give a BE 5-6 eV higher), though kinetic measurements discussed elsewhere indicate that it is probably present as a low-concentration mobile precursor to the dissociated state [20]. Thus the adsorbed oxygen is both dissociated and apparently highly negatively charged both below and above $\theta = 0.5$, even though the Fe atom only takes on full ionic character above $\theta = 0.5$. This is explainable in terms of a cooperative donation of electrons from the (many) Fe substrate atoms to the (few) electronegative O atoms prior to the coverage stage where nucleation into macroscopic islands of Fe oxides becomes significant.

The $c(2\times2)$ and the (1×1) LEED structures observed would, for perfect ordering, correspond respectively to θ = 0.5 and 1 at their maximum intensities. It would be desirable to demonstrate that the conversion from an ideal $c(2\times2)$ structure (where every other site is filled with oxygen atoms) to (1×1) two-dimensional islands of "FeO" (where every site is filled with O atoms) corresponds to the observed conversion of metallic Fe character to Fe³⁺ character. Unfortunately this is not the case. Both LEED structures occur and fade before the emergence of the Fe³⁺ in XPS (see the LEED data of Fig. 10 and the XPS data of Fig. 9). Their maximum intensities, according to our coverage estimates of about 0.2 and 0.4 monolayer, imply that they represent islands that never cover much of the metallic surface. Presumably it is the disordered oxide phase succeeding the (1×1) structure that gives rise to the XPS Fe3+ feature. Therefore, either the $c(2\times2)$ and the (1×1) structures do not contain Fe atoms that are significantly different electronically from metallic Fe (despite the geometric resemblance of the (1×1) to FeO [32]), or they are never present in sufficient quantity on the surface to be distinguished in the Fe(2p) XPS. It should be noted that even if our coverage estimates are incorrect, the conclusion that neither of the LEED structures gives rise to the chemically shifted Fe³⁺ state is unaltered.

We now turn to the low temperature oxygen adsorption on Fe(100). In the present work no attempt was made to study the behavior as a function of coverage, the substrate merely being subjected to a sufficiently large dose of oxygen (several langmuirs) to reach saturation. The O(1s) spectrum corresponding to this situation is shown in Fig. 11, trace (b). Saturation adsorption at 76 K on Fe films produces approximately monolayer adsorption, according to Horgan and King [31], and it is therefore from the Fe($2p_{3/2}$):O(1s) ratio at 123 K that the coverage calibrations are established in the last column of Table 1. After leaving the sample to stand in a flowing atmosphere of 6.7 \times 10⁻⁵ Pa O₂ for 10 min, the extra O(1s) structure shown in Fig. 11(c) is obtained. This was identified as being due

to condensed CO₂ by the value of its O(1s) BE, by the presence of a C(1s) feature at 291 eV, and by the intensity ratio of these peaks. In the UPS all the molecular CO, valence levels could also be observed at their expected energies. The CO₂ was probably generated by the interactions of the oxygen with ion-gauge and other filaments. The pickup of condensable impurities at low temperature is always a potential problem. Carbon dioxide impurities have been identified in a number of previous publications, and in at least one study the unrecognized presence of H₂O has led to misinterpretation [33]. In a previous study of Fe films with O₂ [34], we suggest that an O(1s) level at 533.5 eV attributed to oxygen is in fact due to condensed CO₃. It is essential when taking UPS valence level data at low temperature to monitor the core-level spectra to avoid misinterpretation of the valence levels. The O(1s) spectrum of Fig 11(c) was also recorded with Al- $K\alpha$ radiation [Fig. 11(a)] so that the CO₂ feature could be more clearly observed in the absence of the Fe Auger peak. At 123 K, the main O(1s) peak is narrow and is located at 530 eV, which is therefore characteristic of dissociated highly ionic oxygen. Again, there is no evidence for molecular oxygen, but the CO, interference in the BE region where molecular O2 would be expected reduces the sensitivity of detection. A previous XPS kinetic study of the adsorption of O₂ on polycrystalline Fe at 76 K strongly suggested the presence of a mobile precursor state (presumably molecular oxygen) to the dissociated chemisorbed state, even though molecular oxygen was not observed in the XPS [20]. A thorough kinetic study on the (100) surface is required to establish whether the same is true here, and if so, to ascertain the upper limit of the molecular oxygen concentration from its nonobservance in the XPS.

On warming to 293 K, the CO_2 O(1s) and C(1s) peaks disappear, but an additional O(1s) feature at ≈ 532 eV appears [Figs. 11(d) and (e)]. The origin of this feature is unclear. It disappears on pumping overnight or on warming for a few seconds to ≈ 373 K. It may be due to oxygen atoms produced by the dissociation of some of the condensed CO_2 on warming, which then remain on the oxygenated Fe surface. Conceivably it could represent a change in the nature of the dissociated chemisorbed oxygen on warming from 123 K to 293 K. Obviously, the low-temperature XPS requires a more thorough study than that presented here, which is reported primarily to provide an approximate coverage calibration and to emphasize the difficulties associated with the presence or production of condensable impurities.

It has been suggested previously, from work on Fe films [20], that the major difference between adsorption at low temperature and at room temperature was the capacity at room temperature, but not at low temperature, of the chemisorbed oxygen atoms to undergo a limited num-

ber of diffusion hops across the surface. In this way, the $c(2\times2)$ structure, in which nearest-neighbor sites are empty, is reached. At low temperature the intermediate $c(2\times2)$ structure could not be formed without the necessary diffusion ability and the (1×1) structure would be built up by essentially random site adsorption. The present LEED results at 123 K on the Fe(100) surface provide support for the above model; the $c(2\times2)$ structure is not observed, but an increase in background intensity (indicating disordered adsorption) and then a decrease is observed prior to the (1×1) structure formation.

• Carbon monoxide adsorption: BE and LEED analyses Examination of Figs. 3 and 4 indicates that a total of four distinct electronic states of adsorbed CO can be recognized. These are labeled I-IV in the figures and in Table 2, which gives the O(1s) and C(1s) BE values.

State I corresponds to dissociation into atomic carbon and oxygen and is present on both the (100) and polycrystalline surfaces. The C(1s) and O(1s) BE values are identical (to within ± 0.2 eV) to those of the impurity carbon and oxygen during the cleaning procedure; they are also identical to those obtained by deliberate production of carbon and oxygen atoms on Fe and other transition metal surfaces by a variety of means, e.g., O_2 on Fe, Ni, Co, etc.; CO_2 and CO on Mo, W [2(d)]. Since there is such a great similarity in dissociated carbon and oxygen BE values on a variety of transition metal surfaces, it is clear that the nature of the metal substrate plays only a minor role in determining the BE values.

At 293 K the amount of dissociation at saturation is greater on the polycrystalline surface than on the (100) surface, as can be readily seen from the C(1s) spectra of Fig. 4. This is compatible with the rougher nature of the surface and the fact that previous He I UPS studies of CO adsorbed on a variety of transition metals have established that Fe occupies a borderline position in the periodic table between dissociative and molecular adsorption of CO at room temperature [17].

The remainder of the adsorption at 293 K is molecular, resulting in state II on the (100) surface and state III on the polycrystalline surface. The assignment of both states to molecular CO is based first on the fact that the *BE* values are well removed from the dissociated values. Second, they are close to C(1s) and O(1s) values found for CO molecular states on Ni, W, Mo, and Ru surfaces, and third, the UPS valence level spectra of both states (not discussed here) are characteristic of molecular CO, showing the usual two peaks corresponding to $5\sigma + 1\pi$ and 4σ orbitals. At this stage any discussion of the nature of differences between states II and III must be speculative, but possibilities are a difference in adsorption site, or in bond length or orientation with respect to the surface. An explanation *only* in terms of different adsorption sites on

Table 2 Binding energies for CO adsorbed on Fe.

State	Temperature (K)	Surface	C(1s) (eV)	O(1s) (eV)
I	293	Fe(100), Fe	282.6	530.2
II	293	Fe(100)	284.6	531.1
III	293	Fe polycrys- talline	285.6	531.6
IV	123	Fe(100), Fe polycrystalline	285.6	532.1

the (100) and polycrystalline surfaces, without any change in bond length or orientation, seems unlikely in view of the fact that such small differences in BE are found from metal to metal for the strongly chemisorbed room temperature molecular state. Interpretation in terms of bond length or orientation differences seems more likely. These can, of course, be caused by changes in electronic factors resulting from changes in the site of adsorption. There have been several UPS studies of the valence levels of adsorbed hydrocarbons where changes in the separation between certain valence levels are claimed to be related to bond length and angle changes of the hydrocarbon [35-37]. The BE differences between state II and state III are an increase in both the C(1s) and O(1s) values for state III, but a decrease by ≈ 0.6 eV in the separation between C(1s) and O(1s) values. This behavior is consistent with that found in a theoretical study of a free CO molecule when the CO bond length is increased by about 0.15 bohr radius a_0 from its equilibrium value of 2.15 a_0 [10]. The agreement may be fortuitous since the calculation does not include any effect of substrate atom(s), but the suggestion is no more tenuous than the similar explanations given for the observed changes in hydrocarbon valence levels [35-37]. Surface vibrational spectra would be extremely useful in further characterizing states II and III. Two groups have recently shown that such spectra, obtained by high resolution low energy electron loss spectroscopy (ELS) can distinguish different types of CO bonding on metal surfaces and may also provide guidance as to what sites are involved [38, 39]. If the idea of a stretched CO bond for state III is correct, it presumably arises from increased back-donation from the substrate into the antibonding $2\pi^*$ CO orbital, thus weakening the CO bonding, which would be compatible with the increased quantity of dissociation on the polycrystalline surface.

The LEED sequence of Figs. 2(a)–(d) shows that there is a correlation between O(1s) and C(1s) intensity and the intensity of the $c(2\times2)$ adsorption LEED spots. At present the data are inadequate to indicate whether the corre-

lation is only with the dissociated species, only with the molecular species, or with some combination of the two. We know that prior to nucleation, oxygen atoms on their own give rise to a $c(2\times2)$ structure, and that carbon atoms can do likewise, as evidenced by the $c(2\times2)$ structures observed during the cleaning procedures. In addition, CO adsorption on Ni(100) (which is entirely molecular) also gives rise to $c(2\times2)$ features [40]. The fact that warming the Fe(100) CO-saturated surface from 293 K to ≈ 373 K produces dissociation of the molecularly adsorbed CO [see Figs. 3 and 4, trace (c)] and at the same time sharpens the $c(2\times2)$ structure could be taken to indicate that order is associated only with the dissociated atoms. This is not convincing evidence, however, since mild annealing would be expected to improve the ordering of the chemisorbed species. Thus a mixture of poorly ordered CO, O, and C, all in $c(2\times2)$ sites at 293 K, would give rise to a better ordered O and C atom mixture if heated to 373 K and then recooled. What is clear is that, unlike the case of oxygen at 293 K, where adsorption continues beyond the $c(2\times2)$ stage (causing the $c(2\times2)$ structure to fade rapidly), the adsorption of CO at 293 K does not show any evidence in LEED of reaching a stage where the $c(2\times2)$ intensity starts to decrease. Thus the LEED evidence is that CO adsorption does not cause any significant nucleation into (1×1) islands and does not proceed beyond half-monolayer coverage. This is supported by the relative coverage estimate in Table 1, which indicates 0.2 monolayer of CO as the saturation value. If dissociation were complete this would correspond to a site coverage of 0.4 monolayer. In fact, at 293 K the molecular dissociated ratio is about 3:1, implying a site coverage of 0.15 by CO molecules, 0.05 by C atoms and 0.05 by O atoms. There is an initial contamination of about 0.05 by C atoms, which gives a total θ of 0.3 monolayer. [Note that even if the estimates were based on Scofield's σ values and an assumed L_e value instead of the calibrated value relative to oxygen, the site coverage would only be 0.5 monolayer, and this is still compatible with the LEED data.] The reason for cessation of CO adsorption at less than half coverage without any significant nucleation into the close-packed (1×1) islands is clearly connected with the stability of the CO bond toward dissociation by a partly covered Fe(100) surface, in contrast to the oxygen adsorption case where no molecular chemisorbed oxygen is ever observed on the surface.

For adsorption of CO on Ni, Pd, and Cu (the last at low temperature), previous LEED investigations have identified three broad regions of adsorption, though there are significant detailed differences from metal to metal [40–43]. These regions represent disordered molecular adsorption below $\theta \approx 0.4$ –0.5, $c(2\times2)$ ordered molecular adsorption at and near $\theta=0.5$, and compression structures between $\theta\approx0.5$ and saturation, which apparently ap-

proaches $\theta=0.6$ –0.7. The present work on Fe is complicated by the presence of the dissociated phase, but no similar sequence of regions is observed. A $c(2\times2)$ order is observed from the start of adsorption, but as stated above this could be due to the dissociated species only. No splitting of the $c(2\times2)$ spots characteristic of compression structures was observed near saturation coverage, but this is hardly surprising since that coverage at 0.2 is considerably lower than the 0.6–0.7 values found for Ni, Pd and Cu. In addition Tracy [40–42] repeatedly makes the point that all the possible adsorption structures will not be observed unless the surfaces are scrupulously clean, but for Fe(100) the CO dissociation at 293 K provides its own "contamination."

Adsorption of CO at 123 K (Figs. 5 and 6) gives rise to an additional molecular state, IV, which is apparently the same or very similar on both the (100) and polycrystalline surfaces. The initial adsorption at this temperature is into states II [Fe(100)] and III (polycrystalline Fe) with dissociation into state I almost negligible. Additional adsorption then takes place into state IV, which saturates at a total coverage of $\theta \approx 0.6$ molecule (Table 1). Thus the number of molecules in state IV at 123 K is about twice that in states I and II at 293 K. State IV is reversibly adsorbed; warming to 293 K causes desorption. Re-adsorption can be achieved by cooling and re-exposing to CO. The heat of adsorption of state IV is thus considerably lower than those of II or III. Again, interpretation of the bonding characteristics of state IV is speculative at this stage without proper evaluation of the UPS valence level spectrum and other data, such as the vibrational spectrum, for guidance. It is noted that the C(1s) to O(1s) BE separation is the same as that for state II. If the previous bond-stretching suggestion for state III is to be believed, then state IV, like state II, has a normal CO bond length, as might be expected for a weakly chemisorbed state. Why then are both the C(1s) and O(1s) BE values shifted to higher BE than state II? Again, this seems to be connected with the strength of the chemisorption bond. In a wide variety of molecular adsorption cases it has been generally observed that there is a crude correlation between the adsorption bond strength and the core-level BE values [2(d)]. Thus, physically adsorbed or condensed molecules have higher BE values than chemisorbed states of the same molecules [44]. The reason for this is probably a reduction in final-state relaxation in the weakly adsorbed situation (relaxation always lowers the observed BE[2(c)]) owing to a reduced possibility for metallic substrate electrons to move toward core holes on the weakly held adsorbate. It has been alternatively suggested [45], specifically for CO adsorption, that an apparent correlation between heat of adsorption and O(1s) BE reflects the differing amounts of direct and backbonding contributions to the chemical bond. I would suggest that the correlation between heat of adsorption and BE is capable only of crudely distinguishing very weak from strong adsorption. The correlation may break down when comparing strong adsorption with strong adsorption. For instance, state III has higher BE values than II, but I am claiming that it may represent a state with stronger bonding characteristics than state II.

Low energy electron diffraction on the low temperature state IV was only examined at saturation coverage. Evidence of only a very weak $c(2\times2)$ with a high background structure was found, which suggests that at saturation there is little order in state IV. At lower coverages the situation could be different.

• Comparison of the Fe/CO system with other transition metal/CO systems

An extensive body of literature exists on the XPS and UPS of CO adsorbed at W and Mo surfaces [46-49]. Prior to these measurements it was already known that several different adsorption states existed for which population varied with temperature of adsorption and prior adsorption history. A brief and simplified summary is that there is a strongly adsorbed room temperature state (labeled β); a strongly adsorbed low temperature state (virgin) formed only on a clean and not a previously β -covered surface, which converts irreversibly to β on warming; and a weak reversibly adsorbed state (labeled α for W and γ for Mo) that has a high population at low temperature and a low (W) or zero (Mo) population at room temperature. It was not known prior to the XPS and UPS measurements what the bonding characteristics were for these different states, though there had been much speculation in terms of single bonding, bridge bonding, etc., to substrate atoms. X-Ray photoelectron spectroscopy and UPS were able to distinguish the different states by means of core-level and valence-level BE differences; to demonstrate that the β state is dissociated while the virgin and α states are molecular; and to show that the virgin-to- β conversion represents dissociation. There have also been at least three XPS studies of CO adsorption on Ni [44, 50, 51] though none was very thorough or made on single-crystal surfaces. These, in contrast to the W and Mo results, indicated that only one state (molecular) exists on Ni (at least only one that is resolvable by XPS). One might have expected that the behavior of Fe toward CO would be very similar to that of Ni, since Fe is close to Ni in the periodic table and has generally similar catalytic properties, but different from W or Mo, which have different catalytic properties. From the present results it seems that the opposite is true; Fe exhibits a marked similarity to W and Mo. States II and III are crudely similar to the virgin state, state I is equivalent to the β state, and state IV is similar to the α and γ states on W and Mo. The temperature range for the state populations is different. For W and Mo the β dissociated state dominates at room temperature, whereas for Fe the dissociated and molecular states are of comparable importance, a slightly higher temperature being required for the dissociated state to dominate.

 Comparison with previous electron spectroscopy results on Fe/CO

One previous study of the Fe(100)/CO system using He I radiation has been reported [4]. The authors were able to distinguish dissociative from molecular adsorption by the presence or absence of the atomic O(2p) level at ≈ 5.5 eV. They arrived at the conclusion that adsorption of CO at 300 K caused nearly complete dissociation in contrast to the present results. The reason for the discrepancy in the degree of dissociation is unknown. At 123 K they reported molecular adsorption only, but were unable to recognize the presence of two distinct molecular states at that temperature (II and IV), or that the molecular adsorption had a different character at room temperature (II only).

A previous XPS/UPS study of CO on polycrystalline Fe [3] was able to distinguish between dissociative and molecular adsorption both from the core levels and the valence levels. The authors reported equal amounts of dissociative and molecular adsorption at room temperature, in good agreement with the present results, but at low temperature they did not distinguish between states III and IV. As can be seen from the present results (Figs. 5 and 6), this distinction, though quite feasible, is more difficult than that between states II and IV, where larger BE separations are involved. Yu et al. [52] have also examined CO on polycrystalline Fe, by He I UPS, at room temperature and at 110 K. They observed partial dissociation at room temperature and no dissociation at 110 K, but again did not distinguish between the molecular states at the two temperatures.

There is a very recent XPS/UPS study of CO on Fe(111) at room temperature [53]. On this surface, the authors found that adsorption at low coverage produced entirely dissociated C and O, as judged by their 1s binding energies, and that molecular adsorption followed this. The molecular adsorption comprised about 20 percent of the total CO uptake. Both the increased amount of dissociation compared with the present (100) study and the C(1s) and O(1s) BE values quoted in [53] for the molecular state suggest that the Fe(111) surface behaves toward CO more like polycrystalline Fe than Fe(100).

Conclusions

The XPS and LEED behavior of Fe(100) and polycrystalline surfaces toward CO and O₂ adsorption have been contrasted. There is three times as much CO adsorption at 123 K as at 293 K; a mixture of dissociative and

molecular adsorption occurs in the latter case. The dissociated state, which has a larger population at the higher temperature and a larger population on the polycrystalline surface, is the same on both surfaces. Two qualitatively different molecular states were observed, a strong chemisorbed room temperature state and a weak reversibly adsorbed low temperature state. The strong room temperature state is distinctly different on the (100) and polycrystalline surfaces, as judged by the C(1s) and O(1s) BE values. The differences in BE values are compatible with the state on the polycrystalline surface having a stretched bond compared to the (100) surface. If this were due to an increase in backbonding, with a subsequent decrease in the C-O bond strength, the results would agree with the greater propensity for dissociation on the polycrystalline surface. Low energy electron dissociation indicated c(2×2) adsorbate ordering at 293 K with no evidence for islands being formed with a higher adsorbate concentration (e.g., 1×1 nucleation). It is not yet possible to say whether the ordering refers to the dissociated or molecular species, or both. At low temperature no order is observed at saturation coverage.

The results bear a surprising resemblance to the behavior of CO on Mo or W, rather than on Ni, as might have been anticipated.

Oxygen adsorption produces only dissociated chemisorption, even at 123 K. (It must be remembered, however, that previous kinetic studies have strongly suggested that there is a mobile molecular state that is a precursor of the final dissociated chemisorbed state. Since this is not observed in XPS, its steady state concentration must be low.) Saturation coverage at 123 K is taken as unity, and this value is used to calibrate coverages for the CO and room temperature O, adsorption cases. Low energy electron dissociation at 123 K shows no evidence for significant development of $c(2\times2)$ during adsorption, the pattern changing directly from clean $Fe(1\times1)$ to "FeO" (1×1) at saturation. This is considered to be evidence of reduced mobility of the chemisorbed oxygen atoms at 123 K. At 293 K LEED shows development and then rapid fading of a weak and fuzzy $c(2\times 2)$ structure. The fading is accompanied by development of a (1×1) "FeO" structure that also fades (leaving no order) as adsorption proceeds to a saturation value of about twice that at low temperature. The ideal LEED-derived coverages of $c(2\times2)$ and (1×1) structures at maximum intensity (0.5 and 1 monolayer, respectively) are in disagreement with the coverages derived from the XPS intensity measurements. which give values of ≈ 0.2 and 0.4 monolayer. Because of this and because the $c(2\times2)$ pattern is so poorly developed, it is suggested that neither the $c(2\times2)$ nor the (1×1) structure covers much of the surface before the epitaxial relationship with the substrate is lost. Though it is believed that the (1×1) islands have a geometry very similar to FeO, the XPS Fe(2p) spectrum at the point where the (1×1) pattern is best developed shows no good evidence for modification of Fe from its metallic state. In fact, Fe³⁺ is the only oxidation state positively identified, and only near monolayer coverage [as judged from the O(1s) intensity data], where the (1×1) pattern has almost completely faded. The conclusion is that either the geometric similarity of the (1×1) structure to FeO does not imply any electronic similarity, or that there is never enough of the (1×1) structure on the surface for a chemically shifted Fe(2p) peak to be observed.

In contrast to the case for CO, the Fe/O_2 system is similar to that of Ni/O_2 rather than that of W/O_2 or Mo/O_2 , where adsorption at room temperature ceases near the monolayer point.

No conclusions concerning the detailed geometric structure of these surfaces can be drawn from the data presented here. To do this would require LEED intensity measurements such as have already been made for the full coverage $\text{Fe}(100)/\text{O}_2$ system [32], or simultaneous measurement of surface vibrational frequencies by high resolution energy loss spectroscopy [39].

Acknowledgments

It is a pleasure to acknowledge many helpful discussions with my colleagues, P. S. Bagus, T. J. Chuang, K. R. Wandelt, and H. Winters, and the stimulation provided by a visit from Prof. D. A. King (University of Liverpool, U.K.) during part of this work. K. R. Wandelt is also acknowledged for the initial work with this crystal in devising a cleaning procedure. D. J. Dwyer is thanked for generously providing the Fe(100) single crystal in cut and polished form. I am grateful to J. Goitia for his experimental assistance and to C. F. Brucker and Prof. T. N. Rhodin (Cornell University) for access to their work prior to publication and for discussions concerning it.

References

- 1. J. S. L. Leach, Surface Sci. 53, 257 (1975).
- E. G. Derouane and A. A. Lucas, eds., Electronic Structure and Reactivity at Metal Surfaces, Plenum Press, New York, 1975. (a) T. N. Rhodin and D. Adams, pp. 1, 163, 195. (b) G. C. Bond, p. 537; V. Ponec, p. 523. (c) G. Allan, p. 45; N. D. Lang, p. 81; T, B. Grimley, pp. 35, 113; J. W. Gadzuk, p. 341. (d) C. R. Brundle, p. 389.
- 3. K. Kishi and M. W. Roberts, *Chem. Soc. J. Faraday Trans.* 171, 1715 (1975).
- T. N. Rhodin and C. F. Brucker, Solid State Commun. 23, 275 (1977).
- 5. J. J. McCarroll, Surface Sci. 53, 297 (1975).
- K. R. Wandelt, C. R. Brundle, E. Kay, H. Poenisch, and H. C. Siegmann, Proceedings of the 7th International Vacuum Congress and 3rd International Conference on Solid Surfaces (Vienna, 1977), p. 2153.
- I. P. Batra and P. S. Bagus, Solid State Commun. 16, 1097 (1975).
- I. P. Batra and P. Robaux, J. Vac. Sci. Technol. 12, 242 (1975).
- P. S. Bagus and K. Hermann, Solid State Commun. 20, 5 (1976).

- 10. P. S. Bagus and K. Hermann, Phys. Rev. B 15, 3661 (1977).
- 11. G. Blyholder, J. Vac. Sci. Technol. 11, 865 (1974).
- Chem. Soc. J. Faraday Discuss. 58 (1974). See remarks made by D. R. Lloyd, pp. 136, 137; C. R. Brundle, pp. 135, 137; E. W. Plummer, p. 134; and J. C. Fuggle, p. 136.
- 13. C. R. Brundle, J. Electron Spectrosc. Relat. Phenom. 7, 484 (1975).
- 14. J. E. Demuth and D. E. Eastman, *Phys. Rev. Lett.* **32,** 1123 (1974).
- T. Gustafsson, E. W. Plummer, D. E. Eastman, and J. L. Freeouf, Solid State Commun. 17, 391 (1975).
- P. M. Williams, P. Butcher, J. Wood, and K. Jacobi, *Phys. Rev. B* 14, 3215 (1976).
- G. Broden, T. N. Rhodin, C. Brucker, R. Benbow, and Z. Hurych, Surface Sci. 59, 593 (1976).
- G. Apai, P. S. Wehner, R. S. Williams, J. Stöhr, and D. A. Shirley, *Phys. Rev. Lett.* 37, 1497 (1976), and *Solid State Commun.* 20, 1141 (1976).
- P. M. Marcus, J. E. Demuth, and D. W. Jepsen, Surface Sci. 53, 501 (1975).
- 20. C. R. Brundle, Surface Sci. 66, 581 (1977).
- C. R. Brundle, T. J. Chuang, and K. Wandelt, Surface Sci. 68, 459 (1977).
- 22. C. R. Brundle, M. W. Roberts, D. Latham, and K. Yates, J. Electron Spectrosc. Relat. Phenom. 3, 241 (1974).
- 23. G. W. Simmons and D. J. Dwyer, Surface Sci. 48, 373 (1975)
- 24. C. F. Brucker and T. N. Rhodin, Surface Sci. 57, 523 (1976).
- T. Horiguchi and S. Nakanishi, *Jap. J. Appl. Phys.*, Suppl. 2, Pt. 2, 89 (1974).
- 26. C. R. Brundle, Surface Sci. 48, 99 (1975).
- J. H. Scofield, J. Electron Spectrosc. Relat. Phenom. 8, 129 (1976).
- 28. C. J. Powell, Surface Sci. 44, 29 (1974).
- 29. I. Lindau and W. E. Spicer, J. Electron Spectrosc. Relat. Phenom. 3, 409 (1974).
- I. Lindau, P. Pianetta, K. Y. Yu, and W. E. Spicer, J. Electron Spectrosc. Relat. Phenom. 8, 487 (1976).
- 31. A. M. Horgan and D. A. King, Surface Sci. 23, 259 (1970).
- K. O. Legg, F. P. Jona, D. W. Jepsen, and P. M. Marcus, J. Phys. C 8, 4492 (1975).
- J. E. Demuth and D. E. Eastman, Solid State Commun. 18, 1497 (1976).
- 34. J. K. Gimzewski, B. D. Padalia, S. Affrossman, L. M. Watson, and D. J. Fabian, *Surface Sci.* **62**, 386 (1977).

- T. E. Fischer, S. Kelemen, and H. P. Bonzel, J. Vac. Sci. Technol. 14, 424 (1977).
- T. N. Rhodin, G. Broden, and W. Capehart, J. Vac. Sci. Technol. 14, 425 (1977).
- 37. J. E. Demuth, *IBM J. Res. Develop.* 22, 265 (1978, this issue)
- 38. H. Ibach, H. Hopster, and B. Sexton, Applications of Surface Sci. 1, 1 (1977).
- 39. S. Andersson, Solid State Commun. 21, 75 (1977).
- 40. J. C. Tracy, J. Chem. Phys. 56, 2736 (1972).
- 41. J. C. Tracy and P. W. Palmberg, J. Chem. Phys. 51, 4852 (1969).
- 42. J. C. Tracy, J. Chem. Phys. 56, 2748 (1972).
- 43. M. A. Chester and J. Pritchard, Surface Sci. 28, 460 (1971).
- 44. C. R. Brundle and A. F. Carley, *Chem. Soc. J. Faraday Discuss.* **60**, 51 (1975).
- R. W. Joyner and M. W. Roberts, Chem. Phys. Lett. 29, 447 (1974).
- T. E. Madey, J. T. Yates, and N. E. Erickson, Chem. Phys. Lett. 19, 487 (1973).
- S. J. Atkinson, C. R. Brundle, and M. W. Roberts, Chem. Phys. Lett. 24, 175 (1974).
- 48. S. J. Atkinson, C. R. Brundle, and M. W. Roberts, *Chem. Soc. J. Faraday Discuss.* 58, 62 (1974).
- E. Umbach, J. C. Fuggle, and D. Menzel, J. Electron Spectrosc. Relat. Phenom. 10, 15 (1977), and references given therein.
- P. J. Page, D. L. Trimm, and P. M. Williams, Chem. Soc. J. Faraday Trans. I 70, 1969 (1974).
- R. W. Joyner and M. W. Roberts, Chem. Soc. J. Faraday Trans. 1 70, 1819 (1974).
- K. Y. Yu, W. E. Spicer, I. Lindau, P. Pianetta, and S. F. Lin, Surface Sci. 57, 157 (1976).
- M. Textor, I. D. Gay, and R. Mason, *Proc. Roy. Soc.* (Lond.) A 356, 37 (1977).

Received October 24, 1977; revised December 16, 1977

The author is located at the IBM Research Division laboratory, 5600 Cottle Road, San Jose, California 95193.